

Magnetic-field-assisted electrospinning highly aligned composite nanofibers containing well-aligned multiwalled carbon nanotubes

Lin-Yu Mei,^{1,2} Ping Song,^{1,3} Ya-Qing Liu^{1,3}

¹Research Center for Engineering Technology of Polymeric Composites of Shanxi Province, North University of China, Taiyuan, China

²School of Mechanical and Power Engineering, North University of China, Taiyuan, China

³College of Materials and Science Engineering, North University of China, Taiyuan, China

Correspondence to: Y.-Q. Liu (E-mail: zfflyq98@163.com)

ABSTRACT: Composite nanofiber meshes of well-aligned polyacrylonitrile (PAN)/polyvinylpyrrolidone (PVP) nanofibers containing multiwalled carbon nanotubes (MWCNTs) were successfully fabricated by a magnetic-field-assisted electrospinning (MFAES) technology, which was confirmed to be a favorable method for preparation of aligned composite nanofibers in this article. The MFAES experiments showed that the diameters of composite nanofibers decreased first and then increased with the increase of voltage and MWCNTs content. With the increase of voltage, the degree of alignment of the composite nanofibers decreased, whereas it increased with increasing MWCNTs concentration. Transmission electron microscopy observation showed that MWCNTs were parallel and oriented along the axes of the nanofibers under the low concentration. A maximum enhancement of 178% in tensile strength was manifested by adding 2 wt % MWCNTs in well-aligned composite nanofibers. In addition, the storage modulus of PAN/PVP/MWCNTs composite nanofibers was significantly higher than that of the PAN/PVP nanofibers. Besides, due to the highly ordered alignment structure, the composite nanofiber meshes showed large anisotropic surface resistance, that is, the surface resistance of the composite nanofiber films along the fiber axis was about 10 times smaller than that perpendicular to the axis direction. © 2015 Wiley Periodicals, Inc. *J. Appl. Polym. Sci.* **2015**, *132*, 41995.

KEYWORDS: composites; conducting polymers; electrospinning; functionalization of polymers; mechanical properties

Received 21 October 2014; accepted 12 January 2015

DOI: 10.1002/app.41995

INTRODUCTION

Polymeric nanocomposites with nanoparticles are considered as materials that have the propensity to show amazing mechanical, electrical, and thermal properties due to the interaction between the polymer matrixes and nanoparticles. The carbon nanotubes (CNTs), which consist of cylindrical graphite sheets with nanometer diameter, have come to the research forefront of nanostructural materials due to their interesting properties such as high modulus, optical properties, and electrical/thermal conductivity, since their discovery by Iijima in 1991.¹ In such polymer nanocomposites, interest has grown exponentially in CNTs/polymer nanocomposites since the first polymer nanocomposites using CNTs as filler was reported in 1994 by Ajayan *et al.*² The incorporation of only a few percentages of CNTs into many polymers has led to a significant improvement in mechanical and electrical properties. It is generally believed that the key factors in optimizing the reinforcing effects of CNTs in polymer nanocomposites are the degree of dispersion of the CNTs, their alignment, and the interface adhesion between the CNTs and the polymer

matrixes.^{3,4} Unfortunately, because of their high aspect ratio and strong van der Waals attractions, CNTs is favorable to aggregate, resulting in an inhomogeneous dispersion in polymer matrixes.

An interesting processing method which provides strong elongation of a polymer solution is electrospinning (ES). So ES technology has been shown to be an effective method for improving the dispersion and alignment of CNTs in polymer matrixes.^{5,6} Its feasibility for incorporation of CNTs into nanofibers has been demonstrated in recent works. However, the alignment of nanotubes in the highly aligned nanofibers is still rather seldom. Many methods have been designed to control fiber orientation to obtain aligned nanofibers.^{7–13} Magnetic-field-assisted electrospinning (MFAES) is effective for the fabrication of well-ordered polymeric micro- and nano-fibers over large areas. MFAES possesses several advantages in comparison with other methods. The apparatus of MFAES with just two magnets added to a conventional setup is comparatively simple. The resultant fibers of MFAES present a very good alignment and they can be easily transferred to other substrates.^{14–16}

Polyacrylonitrile (PAN) with good stability and mechanical properties has been widely used as electrospun nanofibers due to their excellent characteristics, such as spinnability, environmentally benign nature, and commercial availability.¹⁷ There are some reports concerning the preparation of electrospun PAN/multiwalled carbon nanotubes (MWCNTs) nanofibers. However, these electrospun nanofibers generally show randomly oriented nonwoven structures and weak alignment. Moreover, the relatively low mechanical strength could finally limit the practical use of composite nanofibers. Therefore, in this article, we reported a highly aligned PAN/polyvinylpyrrolidone (PVP) composite nanofibers containing well-aligned MWCNTs, with the concentrations ranged from 0 to 5 wt %. They were prepared directly by the MFAES technology without any other postprocess. Herein, the mechanical and electrical conductivity properties of the composite nanofibers were also investigated.

EXPERIMENTAL

Materials

The MWCNTs were purchased from Chengdu Institute of Organic Chemistry, Chinese Academy of Sciences (purity: 95%, $-\text{COOH}$ content: 2 wt %, inner diameter: 5–10 nm, length: 0.5–2 μm). PAN powder ($\bar{M}_w=9\times 10^4\text{g/mol}$) and PVP ($\bar{M}_w=1\times 10^6\text{g/mol}$) were supplied by Spectrum China Co. and Shanghai Well-Tone Material Technology Co. The solvent used for dissolving PAN/PVP and PAN/PVP/MWCNTs was *N,N*-dimethylformamide (DMF; Tianjin Fengchuan Chemical Reagent Science And Technology Co.).

Preparation of Spinning Solution

According to the methods from literatures,¹⁸ nonchemical dispersion approach was carried out in three steps. First, PVP was dissolved in DMF to prepare a solution with the concentration of 1 wt %. In the second step, different weights of MWCNTs were dispersed in the PVP/DMF solutions by using a high-power ultrasonic homogenizer (JY92-IIDH; Ningbo, China) for 2 h at 0°C. Finally, the electrospinning solutions were prepared by dissolving 11 wt % of PAN in PVP/MWCNTs/DMF solution under magnetic stirring for 24 h. The calculated MWCNTs concentrations for each component of the various samples were 0, 0.5, 1, 2, and 5 wt % (mass ratios to polymers).

MFAES of Composite Nanofibers

Figure 1 is a schematic illustration of the apparatus used in the MFAES process. Two bar magnets (7.7 cm \times 1.7 cm \times 5.7 cm) were introduced into the conventional collecting region. The magnetic field at the center of the gap was maintained at 0.24 T, and the optimal distance between the two magnets was 2.6 cm. The plastic syringe (20 mL), containing spinning solution, was fitted with a steel needle, which has a plane tip with an inner diameter of 700 μm . The needle was connected to a high-voltage power supply (DW-P503-IACDF; Tianjin Dongwen High-Voltage Power Supply Co.). The feeding rate of the PAN solution into the tip was set at 1 mL/h, using a syringe pump (KDS LEGATO 200; Microplus Technology [Shanghai] Instrument Co.). The distance between the tip of the needle and the collector was 14 cm. The MFAES of hybrid nanofibers was performed at $22 \pm 2^\circ\text{C}$ and relative humidity of $25 \pm 5\%$. The composite nanofibers with different MWCNTs concentra-

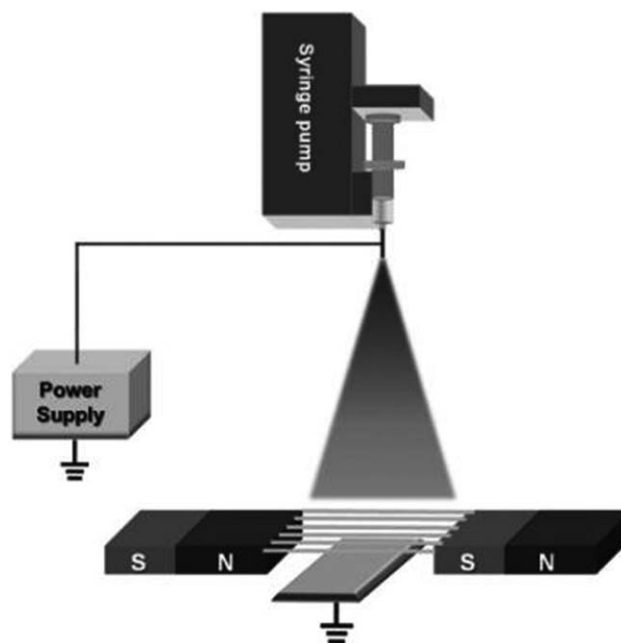


Figure 1. Schematic illustration of the setup used in the MFAES method.¹⁵

tions of 0, 0.5, 1, 2, and 5 wt % were marked as MNF-0, MNF-0.5, MNF-1, MNF-2, and MNF-5, respectively.

Measurement and Characterization

The morphology of the electrospun nanofibers was examined by scanning electron microscope (SEM, SU-1500; Japan) under the magnification of 5000X. The degree of alignment of nanofibers and the average diameter were measured by analyzing the SEM micrographs with Image J software. In this study, the angle (θ) between the long axis of the nanofibers and its expected direction (parallel to the vectors of the magnetic field) was used as the parameter to quantify the alignment. Sixty angles were measured for each SEM micrograph, and the number of nanofibers showing alignment within specific ranges of angles was counted. The degree of alignment of nanofibers is defined as the ratio of the number of nanofibers, whose θ is between -5° and 5° , to the total number of nanofibers. The orientation of MWCNTs in the hybrid nanofibers was characterized by transmission electron microscopy (TEM, JEM1200EX; Japan). X-ray diffraction measurements were conducted by Bruker D8 Advance diffractometer equipped with a diffracted beam monochromator (operating at 45 kV, 40 mA with Cu- $K\alpha$ radiation). The dynamic mechanical analysis (DMA) of the PAN/PVP and PAN/PVP/MWCNTs was carried out with a dynamic mechanical analyzer (METTLER DMA/SDTA 861; Switzerland) with a heating rate of $3^\circ\text{C}/\text{min}$ at a frequency of 5 Hz. The surface resistance was measured by high-resistance meter (ZC36; Shanghai, China) at room temperature and ambient condition. The mechanical properties of the electrospun PAN/PVP/MWCNTs nanofibers were measured on the universal testing machine (SANS CMT6104; Shenzhen, China) at room temperature. The specimens of nanofiber meshes were cut into 1.5×4 cm rectangular shapes. Tensile testing was performed using a 10 N load cell at extension rate of 10 mm/min.

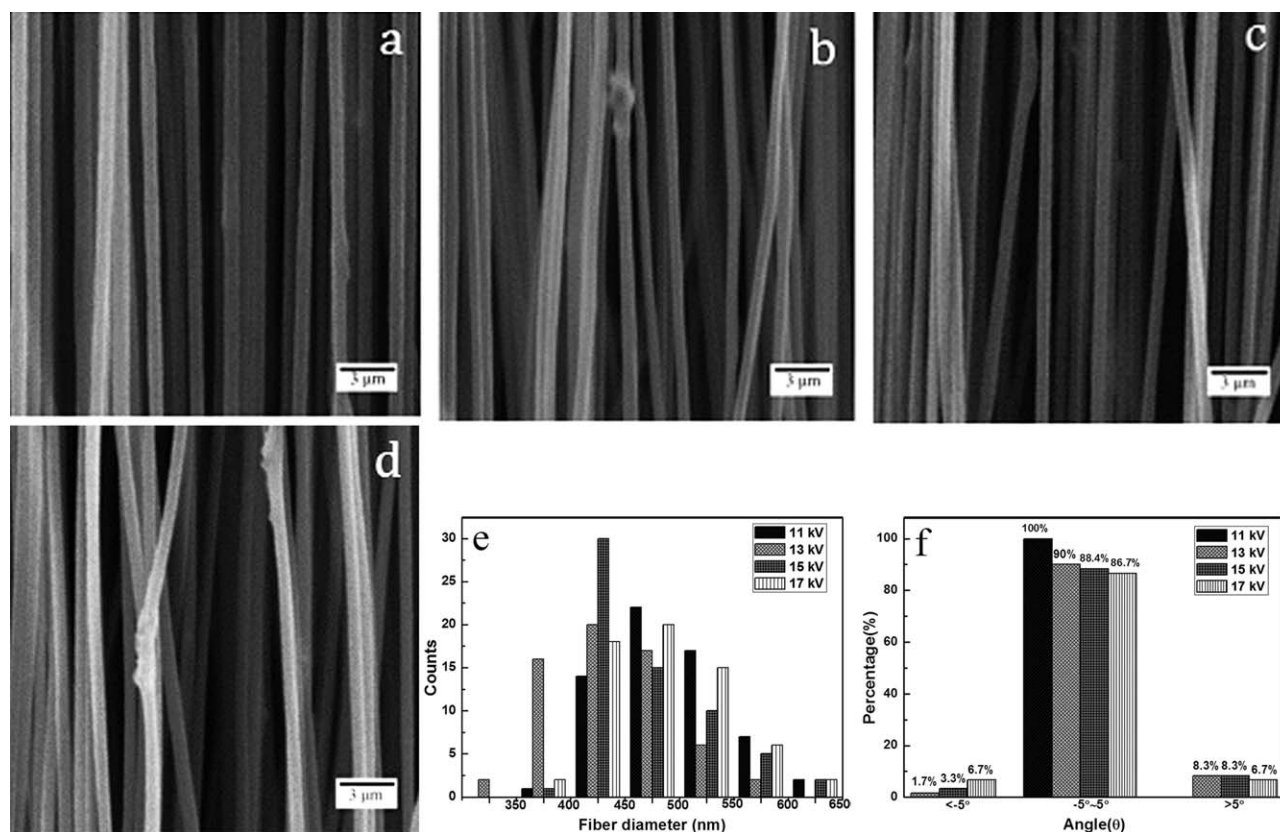


Figure 2. SEM images and corresponding fiber diameter (e) and angle distribution (f) of 1 wt % MWCNTs/PVP/PAN nanofibers under an applied voltage of (a) 11, (b) 13, (c) 15, and (d) 17 kV.

RESULTS AND DISCUSSION

Morphology of Composite Nanofibers

Voltage Effect. Figure 2(a–d) shows the SEM images of the composite nanofibers fabricated at different applied electric voltages. Figure 2(e–f) showed the diameter and angle distribution.

As the voltage increases, the corresponding diameters of the composite fibers are 541 ± 52 , 491 ± 55 , 517 ± 49 , and 531 ± 50 nm, the mean diameter decreases first and then increases. The voltage has two functions, on one hand, a higher voltage was reported to induce more charges on the solution surface and fully stretch the solution jet, which yield more small nanofibers. On the other hand, flow velocity of the jets increased with the voltage increasing, and the traveling time of jets from needle to magnets was shortened, which resulted in larger diameter of fibers.¹⁹ Combined function in the above two aspects would cause the diameter of composite nanofibers to decrease at initial stage and then increase.

At various applied voltages of 11, 13, 15, and 17 kV, the distribution of angle (θ) were shown in Figure 2(f), the degree of alignment of nanofibers were 100, 90, 88.4, and 86.7%, respectively. There were less nanofibers distributing within $\pm 5^\circ$ of the expected direction with increasing voltage. The instability of the jet was enhanced due to the increase of electric field force, and the magnetic force was not enough to suppress the instability of the jet absolutely, which caused the reduction of alignment.

MWCNTs Concentration Effect. Figure 3 displays SEM photographs and corresponding fiber diameter and angle distribution of the electrospun composite nanofibers. The surface of the MNF-0 and MNF-0.5 electrospun nanofibers was very smooth, as shown in Figure 3(a,b). Low surface roughness and unevenness in the MNF-1 and MNF-2 samples were observed, while good alignment in the sample structures still can be seen [Figure 3(c,d)]. However, considerable aggregation and local irregularities were observed as the MWCNTs content increased to 5 wt % [see the sample MNF-5 in Figure 3(e)].

With the concentration of MWCNTs increased from 0 to 5 wt %, the mean diameters of composite nanofibers were 511 ± 52 , 492 ± 58 , 485 ± 58 , 640 ± 62 , and 712 ± 70 nm and the degree of alignment of composite nanofibers were 85, 88.3, 90, 96.6, and 96.6%. In the MFAES process, the solution viscosity and conductivity are two important parameters, which can influence the diameters⁴ and degree of alignment of the composite nanofibers. The viscosity and conductivity increased with the increase of MWCNTs concentration from 0 to 5 wt %. In the processing of MFAES, the charged polymer solution jet was subject to magnet field generated by the magnets and the bending instability of the polymer solution jets can be inhibited by magnetic field. When jets suspended over the gap between the two magnets, the aligned fibers were obtained. With increasing the viscosity, the polymer chains had gotten an improved ability to resist electric field stretching, and the bending instability of jets could be further suppressed, as a result, both the diameter and

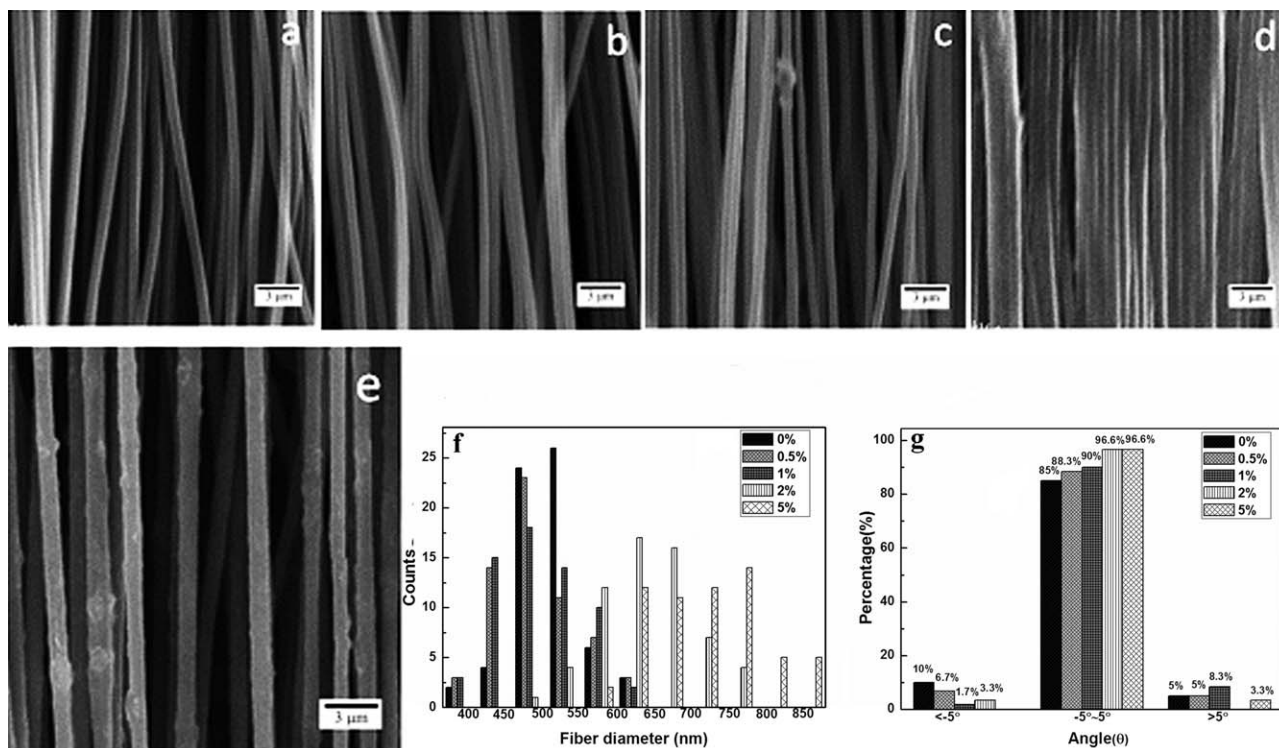


Figure 3. SEM images and corresponding fiber diameter (f) and angle distribution (g) of composite nanofibers under a MWCNTs concentration of (a) 0, (b) 0.5, (c) 1, (d) 2, and (e) 5 wt %.

degree of alignment were increased. With increasing the conductivity, the jets had gotten a greater surface charge density, and the bending instability of jets could be enhanced, so both the diameter and degree of alignment were decreased. The combined effect of viscosity and conductivity made the diameter of composite nanofibers first decrease and then increase, while made the degree of alignment of composite nanofibers increase gradually.

Morphology of Composite Nanofibers Fabricated by Conventional ES and MFAES Methods. The SEM photographs of composite fibers fabricated by conventional ES and MFAES were shown in Figure 4. As shown in Figure 4, the composite nanofibers prepared by conventional ES technology arranged randomly, while it showed a well-aligned nanofibers structure fabricated by the MFAES method. It indicated that MFAES was a favorable method for the formation of aligned PAN/PVP/MWCNTs nanofibers.

TEM Photographs Analysis. TEM were utilized to study the distribution of MWCNTs in the composite nanofibers. Figure 5 shows the TEM photographs of the composite nanofibers. The electrospun nanofibers with the MWCNTs content of 0.5 wt % are shown in Figure 5(a,b). As it can be seen, the MWCNTs in this sample were embedded in the polymer matrix and almost aligned along the fiber axis. However, as the content of MWCNTs increased to 5 wt %, the surface of the nanofibers became irregular and rough, which can be related to the aggregation of MWCNTs and the bundling phenomenon during the MFAES process [Figure 5(c,d)].

XRD Spectra

Figure 6(a) is the XRD spectra for the electrospun PAN/PVP nanofibers meshes. A strong peak was observed at $2\theta = 17^\circ$ and a weak peak at $2\theta = 29^\circ$. These two diffractive peaks can be assigned as (200) and (020) crystal planes of PAN.²⁰ The crystallization nature of MWCNTs was confirmed by XRD studies [as shown in Figure 6(b)].²¹ Peaks indexed to (002), (100), and (101) reflects hexagonal structure at $2\theta = 26.5^\circ$, 43.3° , and 44.2° . The peak at $2\theta = 26.5^\circ$ indicates the typical signal of CNTs or graphite structures. This peak is associated with the (002) diffraction of the hexagonal graphite structure in the carbon materials. Figure 6(c) shows the XRD spectrum of the composite nanofibers. The principal peak of graphene structure at 26.5° does not appear probably because of the high ratio of PAN composite with respect to MWCNTs.²² One peak that can be assigned to the graphene structure at 44.5° is distinguished, corresponding to the (101) plane.

The XRD results suggested that MWCNTs and PAN still retain their crystalline structures in the composite nanofibers. The XRD spectrum of the composite nanofibers had some peaks which stand for impurities.²³ No peaks other than the characteristic peak of PAN and MWCNTs was found in the spectrum of the composite, which meant that there were no new crystalline phase in the composite.

Mechanical Properties. The stress–strain curve in Figure 7 exhibited the relationship of these mechanical variables with the contents of MWCNTs in nanofiber meshes. The close observation of mechanical properties such as tensile strength and

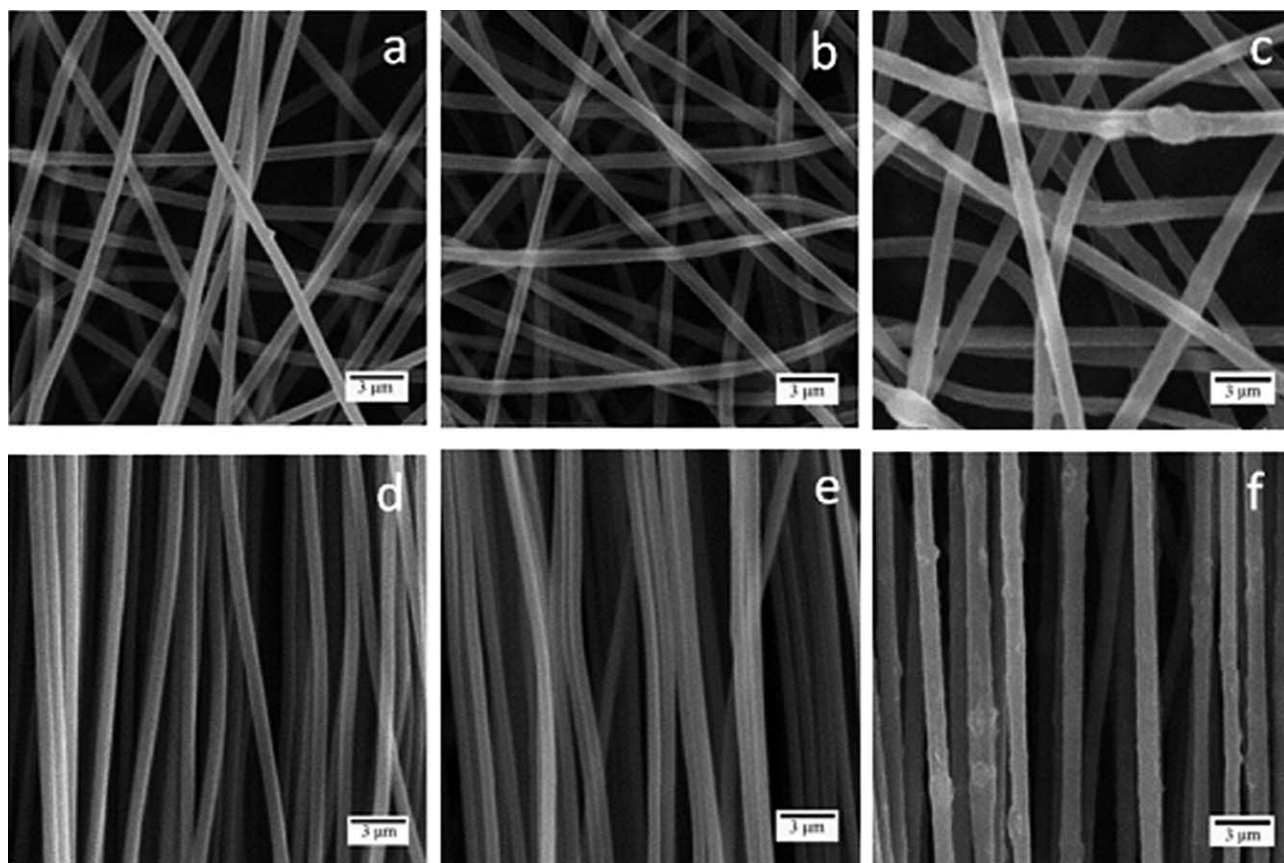


Figure 4. SEM photographs of the composite nanofibers electrospun by conventional ES and MFAES under the MWCNTs concentration of (a, d) 0 wt %, (b, e) 0.5 wt %, and (c, f) 5 wt %.

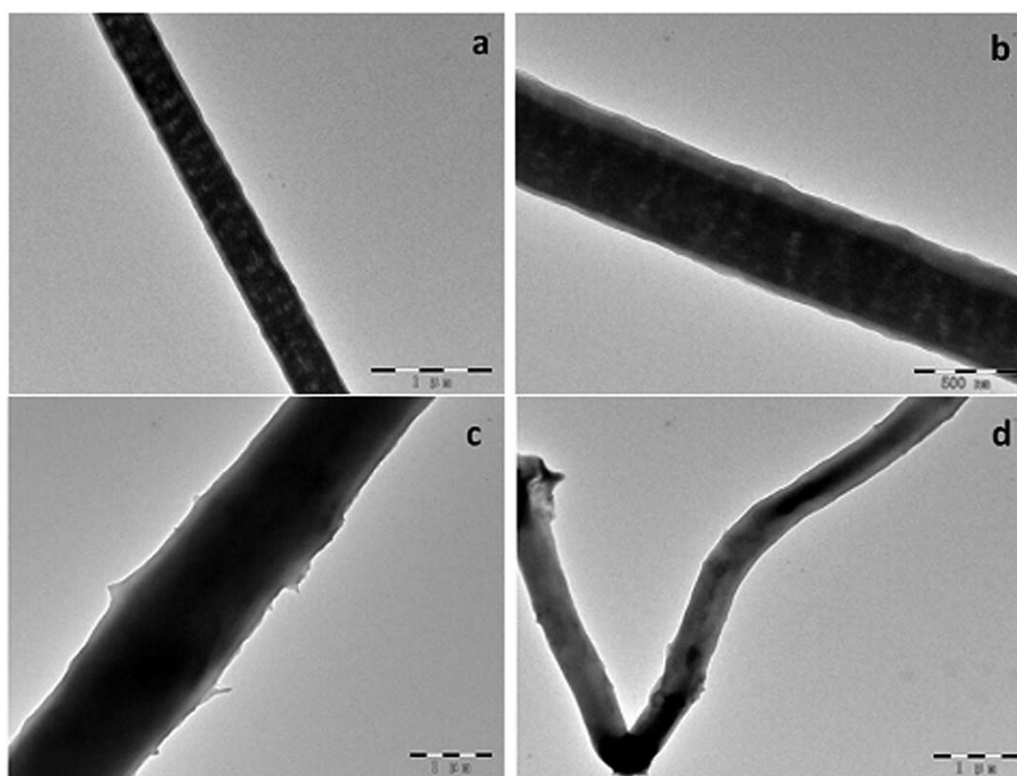


Figure 5. TEM photographs of electrospun nanocomposites: (a, b) MNF-0.5 and (c, d) MNF-5.

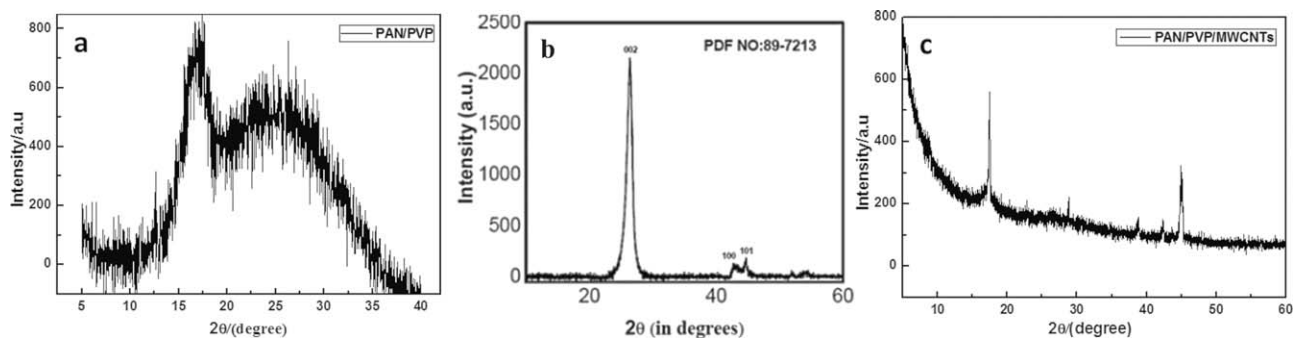


Figure 6. XRD spectra of (a) PAN/PVP, (b) MWCNTs, and (c) PAN/PVP/MWCNTs nanofibers.²¹

elongation at break for various random and aligned PAN/PVP/MWCNTs nanofiber meshes were presented in Figure 8. Tensile strength reached maximal values when the content of MWCNTs was 2 wt %. For random nanofiber meshes, the elongation at break emerged a reduction with the increase of MWCNTs in polymer matrix. For aligned nanofiber meshes, the elongation at break first increased and then decreased.

In the case of the tensile strength, the data presented in Figure 8(a) suggested a significant improvement from 12.73 to 14.25 MPa for a1 and a, from 15.16 to 16.93 MPa for b1 to b, from 19.83 to 21.11 MPa for c1 to c, from 26.92 to 39.68 MPa for d1 to d, and from 23.84 to 25.52 MPa for e1 to e, with the biggest increase of 47%.

There was no doubt that the dispersion of MWCNTs in the polymer matrix was the most important factor in determining the reinforcement effects of MWCNTs for the composite PAN/PVP/MWCNTs nanofiber meshes. As described above, MWCNTs were well aligned along the polymer nanofiber axis under the content below 2 wt %, while they partly or completely crooked above the content of 2 wt %. Therefore, the

mechanical properties of the composite nanofibers were gradually increased from a1 and a meshes to d1 and d meshes, and decreased for e1 and e meshes. The alignment degree of nanofibers also had a profound effect on the mechanical properties of the electrospun meshes. For random-oriented PAN/PVP nanofiber meshes, the combination of adding MWCNTs and ordered array made the tensile strength of PAN/PVP/MWCNTs composite nanofiber meshes increase significantly, up to the maximum of 178%.

For random-oriented composite nanofiber meshes, the declining of elongation at break for all composite samples, compared with neat sample, was caused most likely by the stiffening of the fibers, which was resulted from several factors, such as the chemical interaction between polymer and the carboxyl groups of MWCNTs, and the secondary interaction, for example, van der Waals bonding between polymer and MWCNTs. This implied that the incorporation of MWCNTs in polymer nanofiber structure generally can give rise to be stronger but fewer flexible nanofiber layers. Moreover, the increase in tensile strength and drop in elongation at break have been also reported by Nasouri,¹⁸ Saeed and Park,²⁴ and Mercader *et al.*²⁵

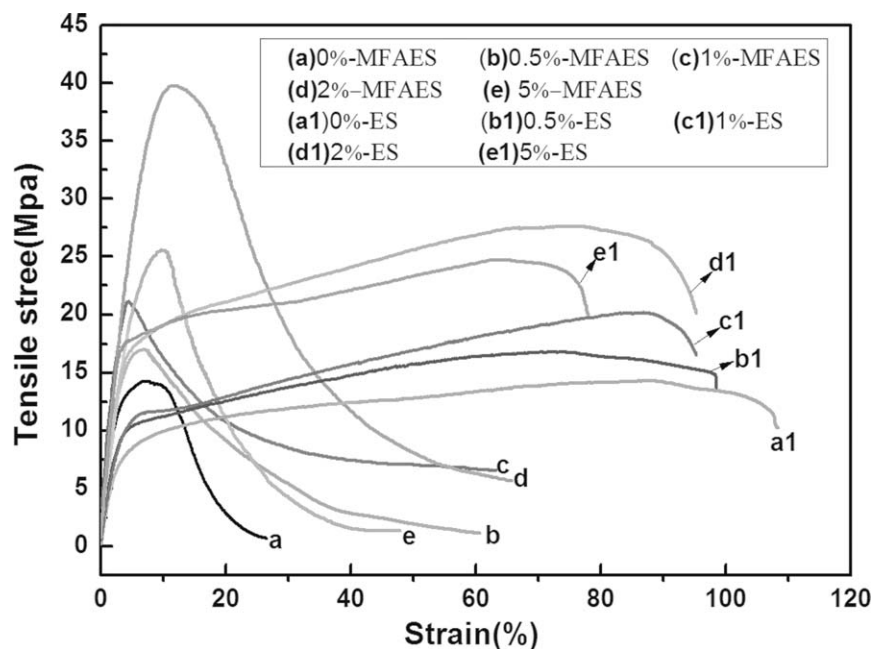


Figure 7. Tensile stress–strain curves of electrospun nanofiber meshes.

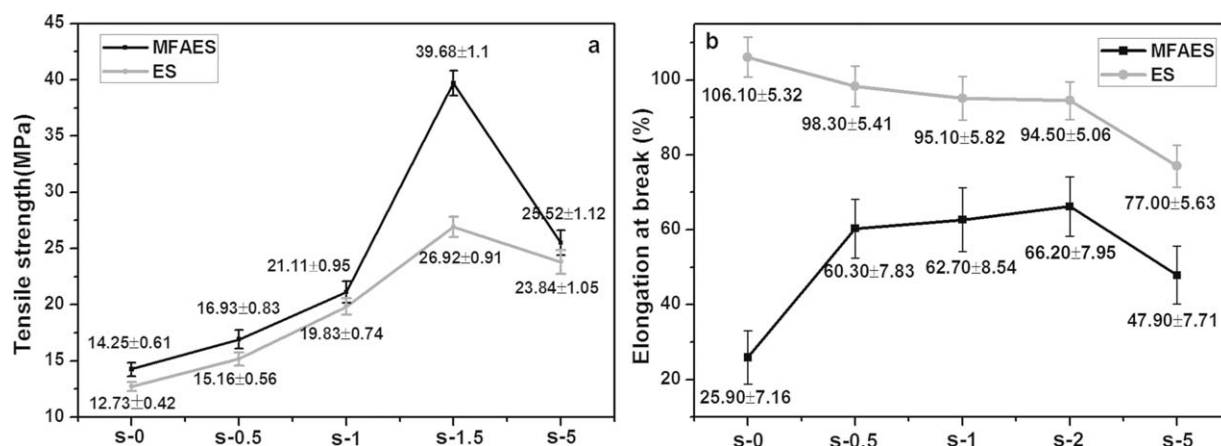


Figure 8. Plot of (a) tensile strength (MPa) and (b) elongation at break (%) as a function of the content of MWCNTs in the composite nanofibers.

For aligned composite nanofiber meshes, the elongation at break first increased and then decreased with MWCNTs content increased. It might be due to the fact that the alignment of MWCNTs in aligned composite nanofibers plays an obvious role of bridging in the course of tension, but the role was not obvious when the MWCNTs were randomly oriented in the composite nanofiber meshes. When the concentration of MWCNTs was 5 wt %, the reunite of the MWCNTs may make the bridging effect became weaker, which caused the downward trend the elongation at break.

Dynamic Mechanical Behavior

The DMA results of the temperature sweeps for the different samples are shown in Figure 9. Figure 9(a) showed the storage modulus curves of PAN/PVP and PAN/PVP/MWCNTs. The storage modulus of PAN/PVP was enhanced by the addition of MWCNTs over the temperature range from 40 to 200°C. Reinforcement was better at low-temperature regions than high-temperature regions. For the concentration rising to 2 wt %, the storage modulus of composite nanofiber mesh reached a maximum, which was 3.5 times of PAN/PVP nanofiber mesh.

The glass transition temperature of PAN [defined here as the peak of the loss modulus curve, Figure 9(b)] seems to shift

slightly to higher temperatures upon further loading of MWCNTs (except 5 wt %). The loss factor peak of the MWCNTs composites [Figure 9(b)] decreases with MWCNTs loading (except 5 wt %), which reflects the reduction in the damping for samples with greater MWCNTs concentrations. This shifting of the loss tangent peaks to higher temperatures for the increased concentration of MWCNTs was attributed to the enhancement of a restricted-mobility of the polymer chains.^{26,27}

For both storage modulus and glass transition temperature, the patterns between them and concentration of MWCNTs resulted in an exception when the concentration was 5 wt %. This is because the dynamic mechanical behavior is strongly dependent on the level of dispersion-distribution of MWCNTs.

Surface Resistance

The surface resistance of PAN/PVP nanofiber meshes was even bigger than $1 \times 10^{15} \Omega/\text{square}$, which was thought to be completely insulated. Because MWCNTs had superb electrical properties, we expected a better electrical conductivity in PAN/PVP/MWCNTs nanofiber meshes. As observed in Figure 3, the composite nanofibers were aligned preferentially along the magnetic field lines. We measured the surface resistance parallel and perpendicular to the fiber axis, respectively.

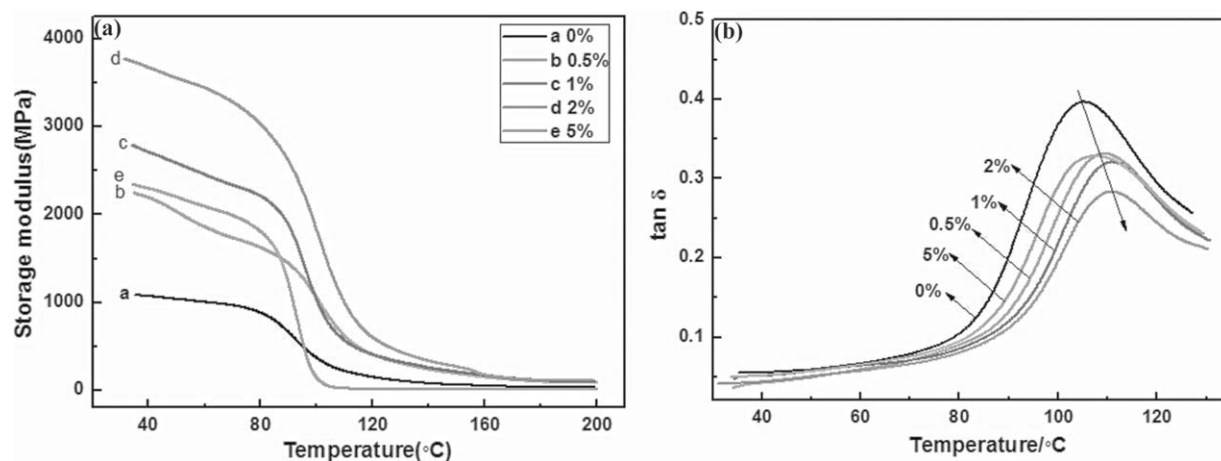


Figure 9. The storage modulus (a) and loss factor (b) versus temperature curves of PAN/PVP and MWCNTs/PAN/PVP nanofibers.

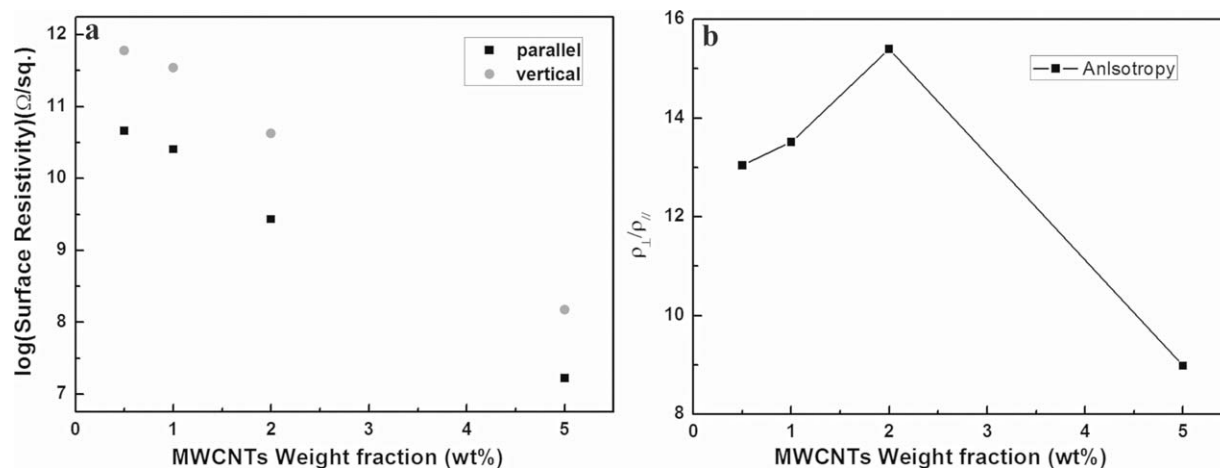


Figure 10. Surface resistance of nanofiber meshes (a) and the anisotropy (b) as a function of MWCNTs concentration.

Because of the excellent electrical conductivity of MWCNTs, the surface resistance gradually decreased with increasing the content of MWCNTs in composite nanofibers. Among the different contents of MWCNTs from 0.5 to 5 wt %, the resistance varied from approximately 1×10^{12} Ω/square to 1×10^7 and 1×10^8 Ω/square for parallel and perpendicular to the fiber axis [as shown in Figure 10(a)]. Because MWCNTs are aligned preferentially along the nanofiber axis and provide good conductivity pathways, we expected a smaller resistance along the nanofiber axis.³ The gradual decrease of the resistance in both directions suggests that the percolation limit was not reached even at 5 wt % of MWCNTs concentration. This value is relatively larger than the typical CNTs concentration for percolation limit of bulk polymer. This could be attributed to the insufficient dispersion and without purification of MWCNTs in our samples.^{28,29}

In addition, the significant distinction in resistance was observed between perpendicular and parallel directions for hybrid nanofibers, as shown in Figure 10(b). The parallel component of the resistance of the composite nanofiber mesh decreased about 10 times than that of perpendicular component, regardless of the MWCNTs concentration. The largest anisotropy was up to 15.4 when the MWCNTs concentration was 2 wt %. This illustrated that both the orientation of MWCNTs and composite nanofibers made the parallel component of resistance of composite nanofiber meshes drop significantly.⁴

CONCLUSIONS

In summary, PAN/PVP/MWCNTs composite meshes of highly aligned nanofibers containing different concentrations of MWCNTs were successfully fabricated by MFAES technology. The experiment demonstrated that the voltage and MWCNTs concentration had significant effects on the diameter and ordering degree. MFAES had proved to be a favorable method for the formation of aligned PAN/PVP/MWCNTs nanofibers. TEM images showed that MWCNTs were almost aligned along the electrospun nanofibers. By increasing the amount of MWCNTs in composite, the surface roughness of nanofibers was increased. After moderate addition of MWCNTs (≤ 2 wt %), the obvious improvement in the tensile properties of PAN/PVP nanofibers

along the fiber axis was shown and the storage modulus of PAN/PVP/MWCNTs composite nanofibers was significantly higher than that of PAN/PVP nanofibers. It is also found that the surface resistance was highly anisotropic, that is, the surface resistance parallel to the fiber axis direction was about 10 times smaller than that perpendicular to the axis direction. The largest anisotropy was up to 15.4 when the MWCNTs concentration was 2 wt %. Therefore, it was suggested that aligning MWCNTs in aligned polymer nanofibers could improve their mechanical property as well as electrical conductivity.

ACKNOWLEDGMENTS

The authors thank Dr. Congyun Zhang and Dr. Shaofeng Zhou for their helpful suggestions and useful comments on the article. Also, they gratefully acknowledge the financial support received from the Youth Foundation of the North University of China (2012) and the project of graduate innovation of Shan Xi province (20133102).

REFERENCES

- Iijima, S. *Nature* **1991**, *354*, 56.
- Ajayan, P. M.; Stephan, O.; Colliex, C.; Trauth, D. *Science* **1994**, *265*, 1212.
- Shao, S.; Zhou, S.; Li, L.; Li, J.; Luo, C.; Wang, J.; Li, X.; Weng, J. *Biomaterials* **2011**, *32*, 2821.
- Sui, G.; Xue, S. S.; Bi, H. T.; Yang, Q.; Yang, X. P. *Carbon* **2013**, *64*, 72.
- Mei, F.; Zhong, J.; Yang, X.; Ouyang, X.; Zhang, S.; Hu, X.; Ma, Q.; Lu, J.; Ryu, S.; Deng, X. *Biomacromolecules* **2007**, *8*, 3729.
- McCullen, S. D.; Stevens, D. R.; Roberts, W. A.; Ojha, S. S.; Clarke, L. I.; Gorga, R. E. *Macromolecules* **2007**, *40*, 997.
- Chowdhury, M.; Stylios, G. J. *Mater. Sci.* **2011**, *46*, 3378.
- Tan, J. S.; Long, Y. Z.; Li, M. M. *Chinese Phys. Lett.* **2008**, *25*, 3067.
- Arras, M. M.; Grasl, C.; Bergmeister, H.; Schima, H. *Sci. Technol. Adv. Mater.* **2012**, *13*, 035008.

10. Edwards, M. D.; Mitchell, G. R.; Mohan, S. D.; Olley, R. H. *Eur. Polym. J.* **2010**, *46*, 1175.
11. Moon, S.; Choi, J.; Farris, R. J. *J. Appl. Polym. Sci.* **2008**, *109*, 691.
12. Tong, H. W.; Wang, M. *J. Appl. Polym. Sci.* **2011**, *120*, 1694.
13. Jalili, R.; Morshed, M.; Ravandi, S. A. H. *J. Appl. Polym. Sci.* **2006**, *101*, 4350.
14. Yang, D.; Zhang, J.; Zhang, J.; Nie, J. *J. Appl. Polym. Sci.* **2008**, *110*, 3368.
15. Liu, Y. Q.; Zhang, X. P.; Xia, Y. N.; Yang, H. *Adv. Mater.* **2010**, *22*, 2454.
16. Yang, D. Y.; Lu, B.; Zhao, Y.; Jiang, X. Y. *Adv. Mater.* **2007**, *19*, 3702.
17. Nataraj, S. K.; Yang, K. S.; Aminabhavi, T. M. *Prog. Polym. Sci.* **2012**, *37*, 487.
18. Nasouri, K.; Shoushtari, A. M.; Kafrou, A.; Bahrambeygi, H.; Rabbi, A. *Polym. Compos.* **2012**, *33*, 1951.
19. Sencadas, V.; Ribeiro, C.; Nunes-Pereira, J.; Correia, V.; Lanceros-Méndez, S. *Appl. Phys. A* **2012**, *109*, 685.
20. Hou, H. Q.; Ge, J. J.; Zeng, J.; Li, Q.; Reneker, D. H.; Greiner, A.; Cheng, S. Z. *Chem. Mater.* **2005**, *17*, 967.
21. Anjalin, F. M. *Der Pharma Chemica.* **2014**, *6*, 354.
22. Bavio, M. A.; Lista, A. G. *Scientific World J.* **2013**, *2013*, 387458.
23. Gao, Y.; Wang, Z. j.; Wang, R.; Liang, J.; Wang, L. *J. Mater. Sci. Technol.* **2006**, *22*, 117.
24. Saeed, K.; Park, S. Y. *J. Polym. Res.* **2010**, *17*, 535.
25. Mercader, C.; Denis-Lutard, V.; Jestin, S.; Maugey, M.; Derré, A.; Zakri, C.; Poulin, P. *J. Appl. Polym. Sci.* **2012**, *125*, E191.
26. Ramontja, J. Fabrication, Characterization, and properties of bionanohybrids based on biocompatible polylactide and carbon nanotubes. Ph.D. Thesis, UNIVERSITY OF THE FREE STATE (QWAQWA CAMPUS), South Africa, November **2010**.
27. Eitan, A.; Fisher, F. T.; Andrews, R.; Brinson, L. C.; Schadler, L. S. *Compos. Sci. Technol.* **2006**, *66*, 1162.
28. Meincke, O.; Kaempfer, D.; Weickmann, H.; Friedrich, C.; Vathauer, M.; Warth, H. *Polymer* **2004**, *45*, 739.
29. Ra, E. J.; An, K. H.; Kim, K. K.; Jeong, S. Y.; Lee, Y. H. *Chem. Phys. Lett.* **2005**, *413*, 188.